X-RAY IMAGING OF THE APS STORAGE RING BEAM STABILITY EFFECTS: FROM THE ALASKAN EARTHQUAKE TO UNDULATOR FIELD CHANGES*

A.H. Lumpkin[#], B.X. Yang, C.Y. Yao, and L. Emery
Advanced Photon Source, Argonne National Laboratory, Argonne, IL 60439 USA

Abstract

The Advanced Photon Source (APS) 7-GeV storage ring serves as a national x-ray synchrotron radiation user facility. The stability and beam quality of the electron beam, and hence the photon beams, are monitored continuously by an array of diagnostics. In particular, x-ray imaging techniques are employed in the diagnostics sector of the ring to characterize beam position, size, and emittance. The x-ray synchrotron radiation (XSR) emitted by the electrons as they pass through the field of a dipole magnet is imaged by a pinhole camera. The images are processed by a Datacube MV200 video digitizer, and the results are provided through the EPICS platform. We have detected the effects on the beam ranging from the arrival of shock waves from the Alaskan earthquake of November 3, 2002 to the variation of the undulator fields by the users during their scans. In the latter case, the beam size effects were observed at the submicron level. Examples of beam centroid and size effects will be presented including some due to longitudinal instabilities at elevated stored beam currents.

INTRODUCTION

As a national x-ray synchrotron radiation user facility, the Advanced Photon Source (APS) 7-GeV storage ring must be held to a high performance level [1]. The stability and beam quality of the electron beam, and hence the photon beams, are monitored continuously by an array of diagnostics. The beam orbit stability is predominantly measured by rf beam position monitors (BPMs) [2] while the beam transverse quality issues are assessed by imaging techniques.   In particular, x-ray imaging techniques are employed in the diagnostics sector of the ring to characterize beam profile, beam position, and emittance. The x-ray synchrotron radiation (XSR) emitted by the electrons as they pass through the field of a dipole magnet is imaged by a pinhole camera. The images are processed by a video digitizer, and the results are provided through the EPICS platform. Improvements to the system since commissioning have made it possible to detect submicron effects in a 100-μm beam size. Since the digitizer operates at 30 Hz, we have the potential to see subtle effects in the beam. These have ranged from the arrival of shock waves from the Alaskan earthquake of November 3, 2002, to the variation of the undulator fields during their scans. We noted, in particular, the cycling of

the circularly polarized undulator (CPU) magnetic fields in a run in the Fall of 2002. In addition, we report the beam size effects in the horizontal (dispersive) plane due to longitudinal instabilities encountered during studies at higher stored beam currents such as 120 mA and 200 mA.

EXPERIMENTAL BACKGROUND

The APS facility includes an injector system based on an S-band linac, a particle accumulator ring (PAR) for stacking and damping charge, and an injector synchrotron to ramp the beam energy to 7 GeV plus the 7-GeV storage ring. The storage ring (SR) has an 1104-m circumference and is composed of 40 sectors of a standard lattice. There are a total of 80 dipoles of which 34 are available for x-ray source points and provision for 34 straights for user insertion devices (IDs) and one straight (S35) dedicated for diagnostics of the particle and photon beams. The nominal stored beam current is 100 mA, and this is routinely maintained in top-up operations by one-shot injection of charge every two minutes. The beam stability is monitored by rf BPMs, and the feedback systems reduce the beam jitter to less than 2.5 μm and 1.5 μm for the horizontal and vertical components, respectively, in a 20-Hz bandwidth [2].

The beam quality is evaluated by using the XSR emitted as the electrons encounter the magnet field of the S35 dipole bending magnet (BM). The source is imaged at about 0.86 magnification by using an in-vacuum 4-jaw aperture located 9.0 m from the BM source point. The x-ray information is converted to visible light by a YAG:Ce crystal located 16.63 m from the source point. Two mirrors and two lenses are used to image the beam spot onto a CCD camera. A target grid at the plane of the crystal is used to validate the focus of the system and determine the calibration factor of 6.8 μm/ch and 5.7 μm/ch for the x and y axes, respectively. The pinhole aperture is typically set at 15 μm by 15 μm, and the effective system resolution is about 22 μm in both planes [3].

The video information is processed by a dedicated Datacube MV200 video digitizer and the results are provided through the EPICS platform. The beam images are fit to a Gaussian profile at the video rate. The beam sizes and positions are process variables that can be tracked and archived. With an independent determination of the beta functions and dispersion at the source point, the beam emittance and coupling factor are also calculated, displayed, and archived. Short-term storage of these values at a 1- to 30-Hz rate is possible. Long-term archives use sampling rates of once per minute.

EXPERIMENTAL RESULTS

In the process of daily review of the beam size, position, and emittance data irregular behavior can be noted and targeted for a more detailed analysis as in the first two cases. The third example is from a machine studies case.

Alaskan Earthquake of November 3, 2002

On a quiet Sunday afternoon in November 2002, a beam orbit excursion resulted in limits being exceeded and an abort of the beam for machine protection purposes at about 16:37 hrs. The routine review of the beam motion prior to this loss of beam in Fig. 1 uncovered an unusual pattern/frequency of motion. This centroid motion and a correlated beam size oscillation were also recorded in the fast data logger data of the pinhole images as shown in Figs. 2 and 3, respectively. An inspection of the data shows that the orbit became perceptibly noisy several minutes before the beam loss. There were ~11 oscillations at tens of microns amplitude in a 5-minute period just before the beam loss. Since these were not compatible with signatures of betatron motion or rf difficulties, further inquiries were made to explain the beam loss. It was noted that the Fermi Lab Tevatron also had a beam loss at nearly the same time. One of their operators assigned their observed beam motion to the arrival of the shock waves from the Alaskan earthquake of November 3 (initiated at 16:12:41 CST) [4]. We also found some corroborating information on the U.S. Geological Survey web pages for a seismic detector site in Ann Arbor, Michigan [5]. The compressions of our ring circumference by the shock waves were sufficient to be easily detected by our diagnostics. The p-wave took about seven minutes to arrive in the region, but the more significant seismic detector activity started at 16:32.

Undulator Field Variation Effects

Later in the same month we observed again a small, strange variation in the vertical beam size and calculated emittance. The period in this case was about one hour, and the amplitude was about ± 0.5 μm out of the 43-μm vertical signal. By searching through the process variables for insertion device activity, we noticed the tests of the CPU had involved cycling of the current values and hence fields at this period. A strong correlation in the vertical emittance (beam size) values is seen with this cycling of the magnetic field as determined by a comparison of data shown in Fig. 4 and Fig. 5, the vertical emittance and current readback, respectively. Very little effect was seen in the horizontal emittance.

Detection of Longitudinal Instabilities

Since the x-ray source point is at a dispersive location in the lattice, the energy spread contribution (75 and 45 μm) to the total observed beam size of 140 or 95 μm for the high-emittance and low-emittance lattices, respectively, is a detectable factor. We have commissioned the SR to run stably at 100 mA, but in our studies for higher currents at 120 and 200 mA we have readily detected the growth of the horizontal beam size due to a presumed longitudinal instability as shown in Fig. 6 (stable) and Fig. 7 (unstable). In these cases the onset of the instability was at the 102- to 103-mA regime, and adjustments were made to the rf cavity temperature set points to reduce the higher-order-mode effects.
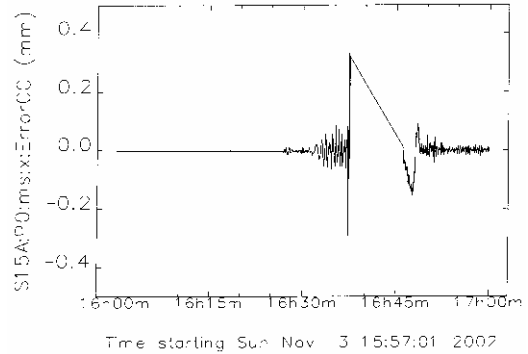

Figure 1: A plot of rf BPM x-position readings at Sector 15 from 1600 to 1700 hours on November 3, 2002. The beam loss was at about 16:37. Beam was restored by 16:50 (fast data logger).
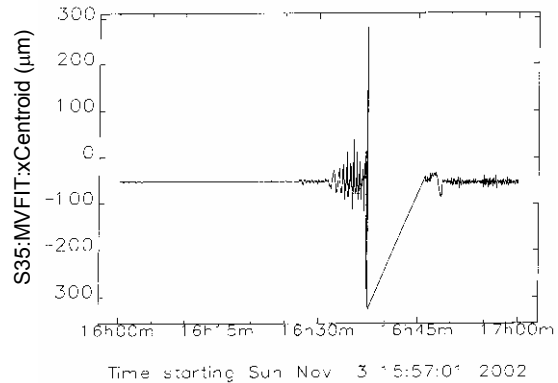

Figure 2: A plot of the x centroid of the pinhole image as processed from Sector 35 from 1600 to 1700 hours on November 3, 2002 (fast data logger).
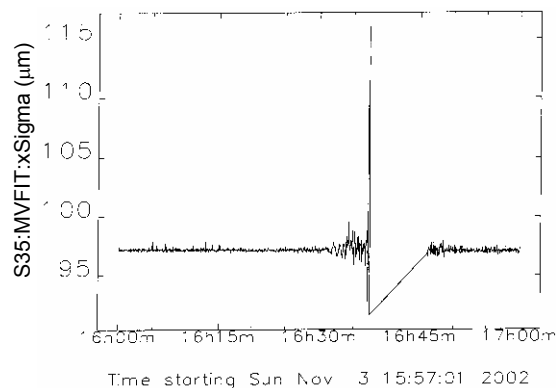

Figure 3: A plot of the x sigma fit results of the pinhole images processed from Sector 35 from 1600 to 1700 hours on November 3, 2002. The oscillations are only a few microns prior to beam loss, but the peaks are aligned with the centroid motion (fast data logger).
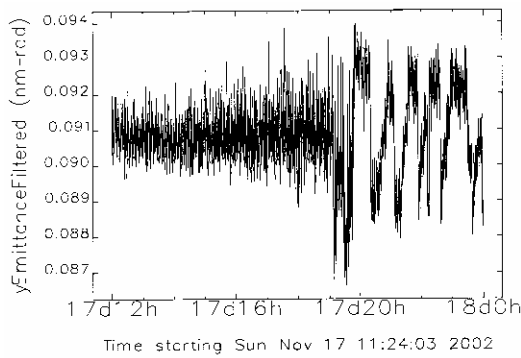
Figure 4: A plot of the y emittance results of the pinhole images processed from Sector 35 from 1200 to 1800 on November 17, 2002. There is a statistically significant beam size oscillation of $\pm$ 0.5 μm with about a 1-hour period.
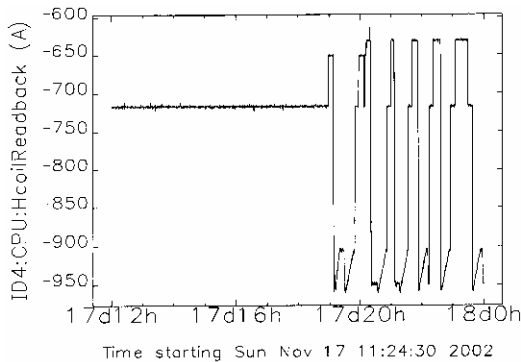

Figure 5: A plot of the Sector 4 CPU horizontal coil readback in A from 1200 to 1800 hours on November 17, 2002. The larger vertical beam emittance/size is correlated with the −650-A value and the smaller value with the −950-A value.

SUMMARY

In summary, the x-ray imaging diagnostics are used not only to validate beam quality, but also to help in identifying the sources of extraneous effects on the beam. These effects ranged from a far-away earthquake to the subtle effects of ID fields varying. The resolution and stability of the diagnostic system have met the challenge. New challenges of supporting lower-emittance lattices with lower vertical coupling are pushing the resolution requirements, so further developments are in the planning stage.

ACKNOWLEDGMENTS

The authors acknowledge the support of O. Singh, G. Decker, and R. Klaffky of the Accelerator Operations Division of APS.
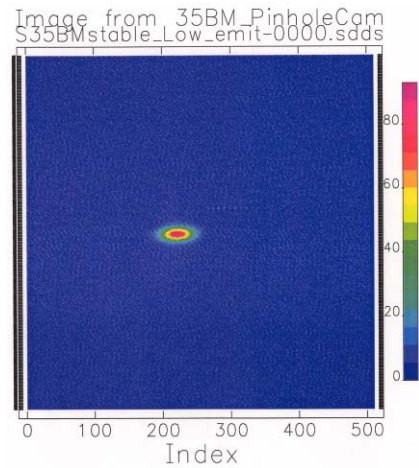

Figure 6: An x-ray pinhole image of the particle beam at S35 in stable condition against a longitudinal instability at 102 mA.
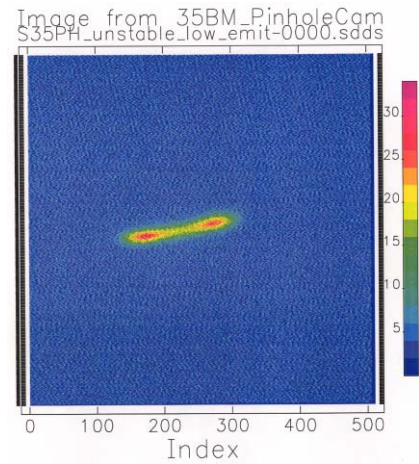

Figure 7: An x-ray pinhole image of the particle beam at S35 in unstable conditions for a longitudinal instability at 103 mA.

REFERENCES

[1] J.N. Galayda, "The Advanced Photon Source," Proc. of the 1995 Particle Accelerator Conference, IEEE, Vol. 1, pp. 4-8 (1996).

[2] G. Decker, J. Carwardine, O. Singh, "Fundamental Limits on Beam Stability at the Advanced Photon Source," BIW 1998, AIP Conf. Proc. 451, pp. 237-244 (1998).

[3] B. Yang, A.H. Lumpkin, L. Emery, and M. Borland, "Recent Developments in Measurement and Tracking of the APS Storage Ring Beam Emittance," BIW 2000, AIP Conf. Proc. 546, pp. 622-630 (2000).

[4] Tevatron Online Status logbook of November 3, 2002, Fermi National Accelerator Laboratory.

[5] Information obtained from the U.S. Geological Survey webpage, http://www.usgs.gov.